

An Insight of *Cryptocarya* Secondary Metabolites as Anticancer P388: Study of Molecular Docking, ADMET Properties, and Molecular Dynamic Simulation**Herlina Rasyid^{1*}, Riska Mardiyanti¹, Ihsanul Arief², Wahyu Dita Saputri³**¹Chemistry Department, Faculty of Mathematics and Natural Sciences, Hasanuddin University, Indonesia²Akademi Farmasi Yarsi Pontianak, Pontianak, Indonesia³National Research and Innovation Agency (BRIN), PUSPITEK, Tangerang Selatan, Banten, Indonesia 15314*Corresponding author email: herlinarasyid@unhas.ac.id**Received** July 14, 2022; **Accepted** February 12, 2023; **Available online** March 20, 2023

ABSTRACT. Secondary metabolites isolated from *Cryptocarya* was known to have various activity especially their cytotoxicity in P388 cell. There were two species of *Cryptocarya* studied in this research that were *Cryptocarya konishii* and *Cryptocarya lucida*. In both species, 8 isolate compounds had bioactivity as anticancer in P388 cells. This study aimed to know the binding affinity and ADMET properties of each isolated compound through P-glycoprotein substrate since this protein was reported to be responsible for the inhibition of P388 cells. Molecular docking was performed using AutoDock4 and AutoDockTools software to know the binding energy and interaction of isolate compounds against the P-glycoprotein substrate. ADMET properties calculation was done using the pkCSM web server for all compounds. Molecular docking results showed that Kurzichalcolactone B (**7**) isolated from *C. lucida* had the lowest binding energy. It resulted in the highest total intermolecular energy from the contribution of van der Waals and hydrogen bond energy. Binding energy calculation using MM-PBSA method revealed a similar result that ligand **7** had a lower binding energy than **5**. Calculation of ADMET properties resulted that some of the isolate compounds fulfilling the minimum standard parameters in ADMET properties.

Keywords: ADMET properties, Anticancer, *Cryptocarya*, Molecular Docking,**INTRODUCTION**

Cryptocarya is a genus who have more than 300 species that are often found around the tropical Asia Pacific (Gangopadhyay & Chakrabarty, 2005) such as Thailand, Malaysia, Singapura, Indonesia dan Australia (de Kok, 2015). *Cryptocarya* is a plant that has many chemical constituents such as alkaloids (Giordano et al., 2019), pyrones (Liu et al., 2015), flavonoids (Nehme et al., 2008), terpenoids (Siallagan et al., 2008), dan chalcone (Fera Kurniadewi et al., 2010).

Cryptocarya has been known and used by the community as a traditional medicine to treat liver diseases and rheumatism (Giordano et al., 2019). Secondary metabolites in *Cryptocarya* have activities as an anti-inflammatory (Feng et al., 2012), anti-plasmodial (Nasrullah et al., 2013), anti-tuberculosis (Chou et al., 2011), antimalarial (Liu et al., 2015) and also in several studies it was found that *Cryptocarya* has potential as an anticancer (Chang et al., 2016; Ray et al., 2021)

In several studies have been conducted, species of *Cryptocarya* that are reported to contain secondary metabolites that have anti-cancer activity include *Cryptocarya costata* (Usman et al., 2006), *Cryptocarya pulchineria* (Juliawaty et al., 2020),

Cryptocarya konishii (F. Kurniadewi et al., 2017) and *Cryptocarya lucida* (Siallagan et al., 2008)

The results of research conducted by Kurniadewi et al. (2010), found that 7 compounds were isolated from the methanol extract of the wood of the *Cryptocarya konishii* and showed a strong inhibition of the growth of murine leukemia P-388 cells. In *Cryptocarya lucida* there were two compounds found that were Kurzichalcolactone A and Kurzichalcolactone B (Siallagan et al., 2008). There were 8 total compounds isolated from two species of *Cryptocarya* and showed good bioactivity as an anticancer. However, in silico study of those compounds has never been conducted. This study aims to evaluate the binding affinity and ADMET properties of all isolated compounds through molecular docking (Palestro et al., 2014; Rachman et al., 2018) and ADMET calculation (Pratama et al., 2020)

Molecular docking is carried out to study the simulation of the interaction between a chemical compound and macromolecules to predict the active site of a macromolecule and as a guide to design new more active compounds (Kitchen et al., 2004). One important rule in docking study is the main amino acid residue(s) interacting with the native ligand have to

also interact with the proposed or the newly designed compound (Pinzi & Rastelli, 2019).

The properties of ADMET are phenomena that are closely related to how the performance of a chemical compound in the human body. Each of the properties in ADMET will reflect the outcome of a chemical compound when interacting with various organs in the body. Prediction of the ADMET properties of a compound is essential, especially for foreign chemical compounds that are consumed in the long term or at large concentrations (Daina et al., 2017; Pires et al., 2015).

EXPERIMENTAL SECTION

Ligands Preparation

There were 8 compounds isolated from *C. konishii* (Fera Kurniadewi et al., 2010) and *C. lucida* (Siallagan et al., 2008) that were selected as tested ligands (Table 1). The 3D structure of each ligand was downloaded on the PubChem website (<https://pubchem.ncbi.nlm.nih.gov/>) except for desmethylinfectocaryone because of the absence of its structure. Due to the similarity of structure between desmethylinfectocaryone and infectocaryone, so we edited the structure of infectocaryone in Avogadro software (Hanwell et al., 2012) and optimized the structure using the General Amber Force Filed (GAFF) method (Wang et al., 2004).

Molecular Docking

The protein structure used in this research was P-glycoprotein (PDB ID: 6FN1) since this protein is responsible for the inhibition of P388 cancer cells (Gatoillat et al., 2015). Native ligand is obtaining from the complex of P-glycoprotein and numbering as ZQU (Zosuquidar) ligand. Each ligand and protein substrate were prepared to dock using Chimera software by adding hydrogen and optimizing the structure (Pettersen et al., 2004). The grid box size used is 70 x 70 x 70 Å, the grid center size is 152.163;

150.946; 152.534 (xyz coordinate) and the spacing is 0.375 Å. The docking protocol was set to give the 10 best conformations using the Lamarckian Genetic Algorithm that was implemented in the AutoDock4 package (Morris et al., 1998). The best conformation was chosen based on the lowest binding energy value and the visualization of 2D interaction was depicted using Discovery Studio Visualizer program (Dassault Systemes, 2019).

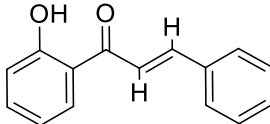
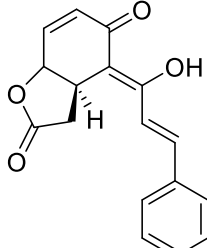
Molecular Dynamic Simulation Protocol

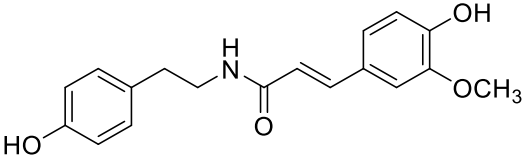
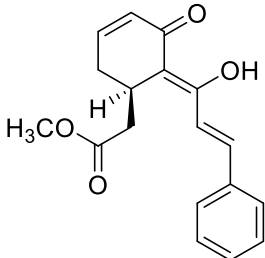
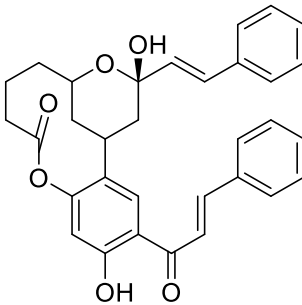
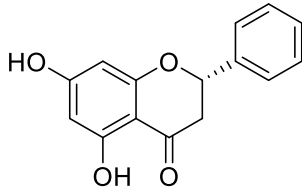
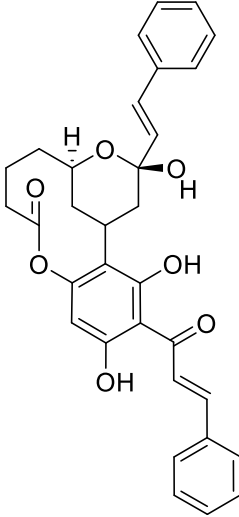
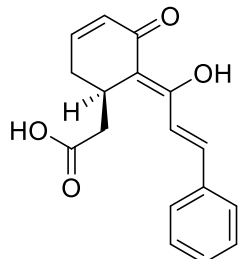
Molecular dynamic simulation was conducted for the complex of ligand 5 and 7 against P-glycoprotein. These both of ligands were chose due to the lower binding energy resulted in molecular docking analysis. Both complexes were compared to the structure of single protein without ligand. MD simulation was done by using YASARA Dynamics program (YASARA Biosciences GmbH, Vienna, Austria) (Land & Humble, 2018). Force field used in this study is Amber14 in a periodic boundary condition (Wang et al., 2004). Temperature and pH of system were set about 310 K and 7.4, respectively (Dash et al., 2019). TIP3P solvent was selected and each complex was added counter ion Na⁺ and Cl⁻ (Mark & Nilsson, 2001). Each complex was run until 10 ns by using time step 0.25 fs. Then, trajectory data used to analyse radius of gyration, RMSD complex, RMSD ligand, RMSF, and MM-PBSA energy.

ADMET Properties Calculation

All of the ligands were converted into smiles format using the Open Babel program (O'Boyle et al., 2011) and then submitted to the pkCSM web server one by one (Pires et al., 2015). Calculate the ADMET properties by choosing the ADMET menu. pkCSM program provided the data including the result of the Lipinski rule of five calculations and adsorption, distribution, metabolism, excretion and toxicity data for each ligand.

Table 1. List of isolate compounds from *C. konishii* (Fera Kurniadewi et al., 2010) and *C. lucida* (Siallagan et al., 2008)

Ligand	PubChem ID	Isolate Compounds	Structure
1	638276	2-hydroxy chalcone	
2	10379026	Cryptocaryone	

3	5280537	Trans-N-Feruloylramine	
4	10379922	Infectocaryone	
5	102331934	Kurzichalcolactone A	
6	68071	Pinocembrine	
7	102331935	Kurzichalcolactone B	
8	-	Desmethylinfectocaryone	

RESULTS AND DISCUSSION

Molecular Docking Analysis

In order to know the binding affinity of ligands, molecular docking analysis is conducted through the AutoDock program. **Table 2** shows the result of docking analysis, and all ligands have low binding energy. Comparison of binding energy between all ligands and native ligand (ZQU) presents that some of ligands have a lower energy. Binding energy results in the AutoDock4 program come from the sum of several energies such as intermolecular, internal energy, and torsional and unbound system energy. Intermolecular energy of each ligand contributes from hydrogen bond, van der Waals, and electrostatic energy.

The more intermolecular interaction is resulting a lower value of binding energy but represents a stronger interaction. **Table 3** presented the interactions between each ligand and P-glycoprotein substrate. Some of interacting residue found in complex ZQU

against the substrate also presents in the interaction of newly ligands such as Trp231, Met875, Gln945, etc. Ligand **5** is an isomer of ligand **7**, it makes the binding energy of these compound similar. These two ligands have a more functional group, furthermore, give a more interactions with the P-glycoprotein substrate and resulting in a lower binding energy compared with the other complex protein-ligand. Two-dimension interaction between ligands **3** and **7** as the complex protein-ligand with a higher and lower binding energy (**Figure 1**). It is implied from **Figure 1** that complex **3** has a higher binding energy value because the less of interaction with the substrate and there was unfavourable interaction with Ala69 residue, despite, ligand **7** having a more interactions such as hydrogen bond (Tyr949, Gln945, and Ile339), van der Waals, pi-alkyl stacking, and pi-pi stacking (Tyr952) making the lower binding energy value.

Table 2. Molecular docking result of ligands through P-glycoprotein substrate

Ligand	Inhibition Constant	Final Intermolecular Energy (kcal/mol)	Final Total Internal Energy (kcal/mol)	Torsional Free Energy (kcal/mol)	Unbound System's Energy (kcal/mol)	Binding Energy (kcal/mol)
		[1]	[2]	[3]	[4]	[1+2+3-4]
1	13.35 μ M	-7.84	-0.57	1.19	-0.57	-6.65
2	1.06 μ M	-9.05	-1.09	0.89	-1.09	-9.05
3	18.32 μ M	-8.85	-1.30	2.39	-1.30	-6.46
4	3.21 μ M	-9.28	-1.56	1.79	-1.56	-7.49
5	26.47 nM	-12.72	-2.86	2.39	-2.86	-10.34
6	8.03 μ M	-7.85	-0.98	0.89	-0.98	-6.95
7	8.25 nM	-13.41	-0.77	2.39	-0.77	-11.03
8	5.56 μ M	-8.96	-0.55	1.79	-0.55	-7.17
ZQU	1.03 μ M	-10.26	0.00	2.09	0.00	-8.17

Table 3. Residue interactions of all ligands in P-glycoprotein substrate

Ligand	Interactions
1	Gln772, Gln837, Ser830, Trp231, Met875, Gln989, Phe302, Phe993, Val834, Ala833, Val990, Ala994, Met298
2	Gln772, Gln837, Asn720, Phe769, Phe302, Ser765, Tyr306, Leu723, Gln724, Trp231, Met298, Val990, Phe993, Gln989
3	Leu64, Glu874, Trp231, Met875, Phe941, Gln945, Tyr949, Pro65, Val62, Gly61, Thr198, Gln194, Gln364, Leu878, Leu235, Ala232
4	Tyr306, Gln989, Ile305, Phe982, Gln837, Gly721, Asn841, Gln724, Leu723, Asn720, Val990, Ala986, Met985, Phe302
5	Ala986, Gln989, Tyr306, Met985, Phe982, Ile305, Gln724, Tyr309, Ser765, Trp231, Phe302, Asn720, Met875, Phe993, Gln837, Gln772, Phe769, Leu723, Met298
6	Gln837, Gln772, Val990, Ala833, Ser991, Val834, Gln989, Phe302, Met298, Phe769, Ala994, Phe993, Trp231, Met875
7	Gln945, Tyr949, Ile339, Glu874, His60, Gln194, Gly61, Ala195, Thr198, Ser343, Gln346, Leu235, Trp231, Ala228, Phe342, Met68, Tyr952, Met948, Met67, Leu64, Ala232, Leu878
8	Gln837, Asn295, Gln772, Ser830, Ala833, Val834, Trp231, Phe302, Phe993, Gln989, Gly773, Met298, Val990, Ala994, Pro995
ZQU	Trp231, Gln945, Met875, Glu874, Met985, Met948, Leu64, Tyr949, Leu878, Ala232

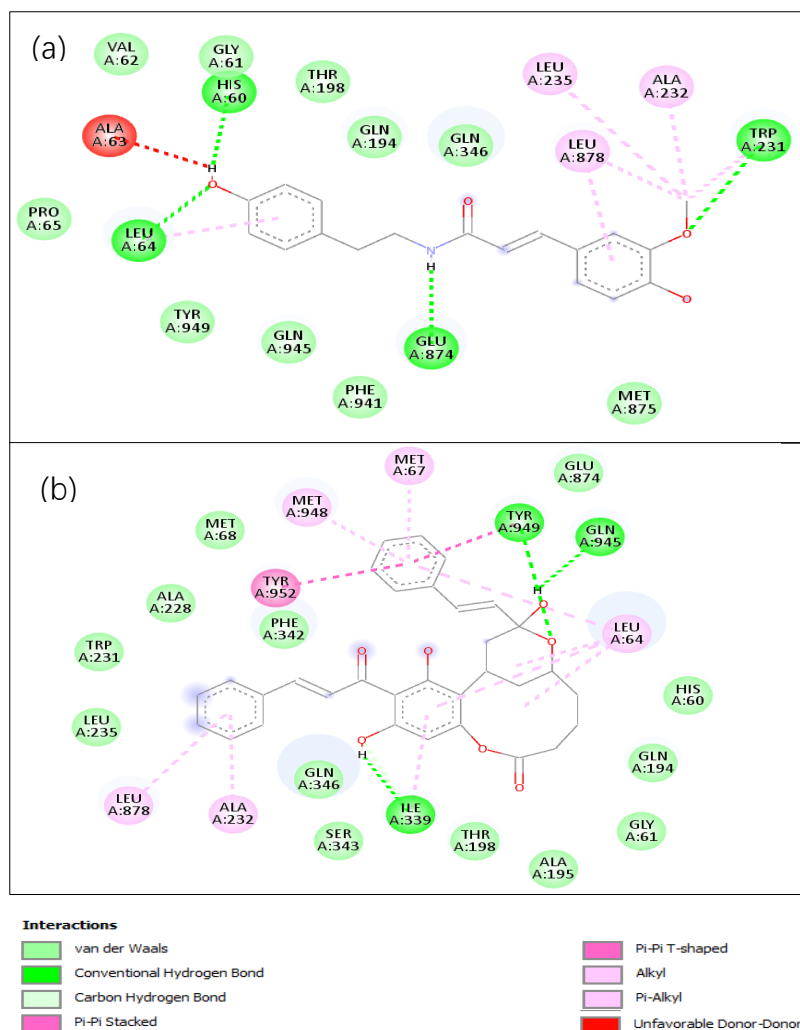


Figure 1. 2D-Interaction of ligands 3 and 7 against P-glycoprotein substrate

Molecular Dynamic Simulation

Molecular dynamic simulation had been conducted to the complex of ligand 5 and 7 against P-glycoprotein comparing with the single protein structure. These both ligands were choosing due to the lower binding energy than the other tested ligand in molecular docking analysis. Radius of gyration is a parameter that describe equilibrium conformation in a whole system. The lower value showed the folded condition of protein structure, and the highest value described the unfolded structure. **Figure 2** showed that addition of ligand to the protein structure could increase the RG pattern specially in the end of simulation time. Addition of ligand **7** to the protein structure give a better condition than ligand **5** based on the folding condition of the P-glycoprotein. It was also confirmed in RMSF graph, fluctuation of some amino acid residues was higher than residue in single protein structure. The RMSD analysis showed that deviation of the single protein structure was around 4-5 Å but addition of ligands could decrease this rmsd value, indicating that this ligand gave a more stability effect to the P-glycoprotein. Comparison of ligand

stability was depicted in **Figure 2d** and showed that ligand **5** was more stable than **7** due to the lower rmsd value. Even though these both of ligands are enantiomer.

$$\text{Binding Energy} = E_{\text{pot}} \text{ Receptor} + E_{\text{solv}} \text{ Receptor} + E_{\text{pot}} \text{ Ligand} + E_{\text{solv}} \text{ Ligand} - E_{\text{pot}} \text{ Complex} - E_{\text{solv}} \text{ Complex} \quad (\text{Eq. 1})$$

Binding energy of ligand 5 and 7 was evaluated using MM-PBSA (Molecular mechanics Poisson-Boltzmann surface area) method based on the Equation 1. MM-PBSA method calculate binding energy from the difference of solvation condition from receptor, ligand, and complex when bound and unbound condition (Miller et al., 2012). **Table 4** showed the similar binding energy both ligands. The structure of both ligands that was enantiomer gave a different potential energy and impact to the solvation energy. The ligand 7 had a solvation energy lower and gave the better binding energy. This result also made a more stable of complex protein ligand between ligand 7 and P-glycoprotein and it was in line with the molecular docking analysis.

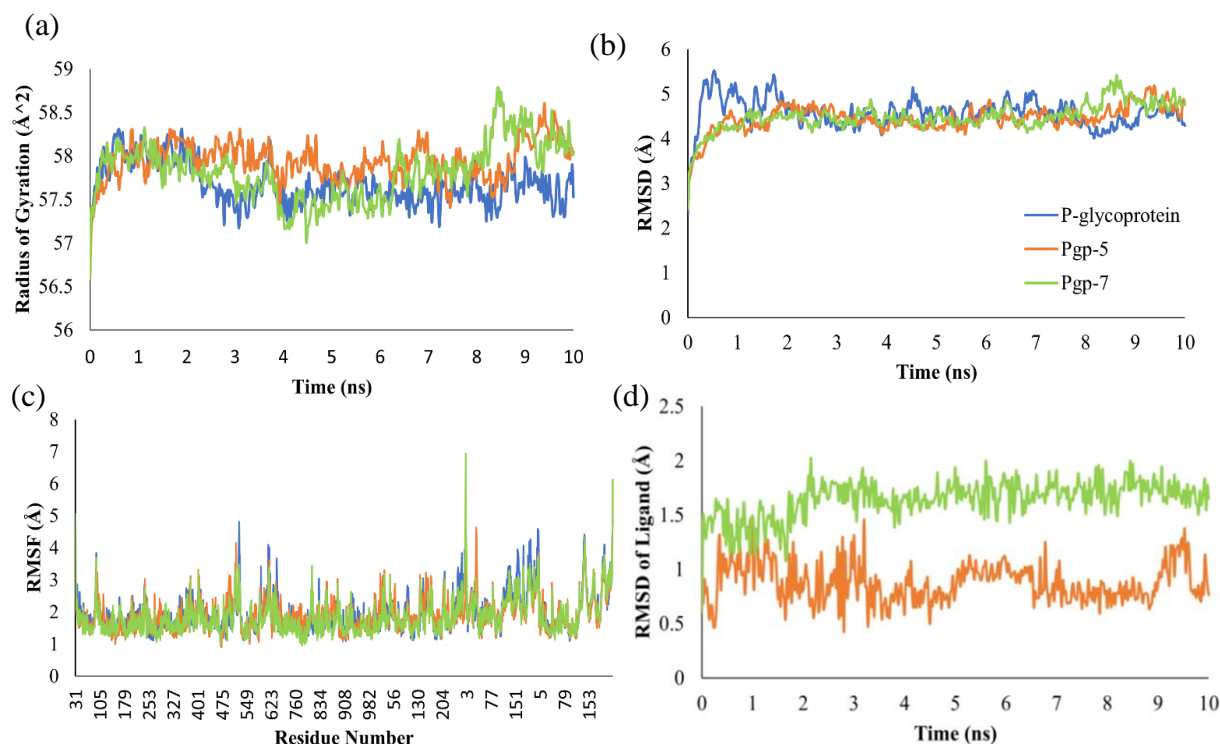


Figure 2. Molecular dynamic simulation result of complex 5 and 7 against P-glycoprotein compared to the single P-glycoprotein (a) radius of gyration, (b) RMSD of ligand, (c) RMSF, and (d) RMSD total graph

Table 4. MM-PBSA energy result of complex 5 and 7 against P-glycoprotein

Energy	5 (kJ/mol)	7 (kJ/mol)
Potential Energy of Receptor	-42055.0	-40236.7
Solvation Energy of Receptor	-116474.0	-118516.0
Potential Energy of Ligand	-41587.1	-39873.8
Solvation Energy of Ligand	-116601.0	-118582.0
Potential Energy of Complex	-42055.0	-40236.7
Solvation Energy of Complex	-116474.0	-118516.0
Binding Energy	-158188.0	-158456.0

ADMET Properties

The result of ADMET properties calculate in the pkCSM web server is present in **Table 5**. In adsorption parameters, ligands 5 and 7 fulfil all the parameters except CaCO_2 permeability. This parameter describes the cell line of human epithelial colorectal adenocarcinoma cells and is considered to have a high CaCO_2 permeability higher than 0.9. The interesting part is only compounds 5 and 7 are considered as P-glycoprotein substrate and P-glycoprotein inhibitor I and II, which supports the result of docking analysis which are those compounds have lower binding energy against P-glycoprotein.

The distribution parameters of ligands are demonstrated by some of parameters. The volume of distribution (VDss) describes the total dose of a drug and considers having a low value ($\log \text{VDss} < -0.15$)

(Pires et al., 2015). Ligands **5-8** show a lower volume of distribution compared to the others ligand indicating that these ligands have a good volume of distribution.

Metabolism parameters of ligands show that all ligands are not suitable as CYP2D6 substrates and are more likely to be CYP3A4 substrates. These two substrates are the main ones responsible for the metabolism process in Cytochrome P450. Ligands **8** presents a poor metabolism process due to a mismatch of all parameters. Renal Organic Cation Transporter 2 (OCT2) is a parameter that describes the disposition and clearance of the drug. In this study, only ligand **4** fulfil this parameter. In the toxicity test, all ligands present non-mutagenic potential based on the AMES toxicity result. Some ligands also present an effect on the skin and liver.

Table 5. ADMET properties of ligands isolated from *C. konishii* and *C. lucida*

Properties		Ligand							
		1	2	3	4	5	6	7	8
Adsorption	CaCO ₂ Permeability	1.422	1.086	0.994	1.057	0.404	1.152	0.404	0.96
	Intestinal absorption	93.429	96.22	88.193	95.196	96.886	92.417	96.886	91.83
	Skin Permeability	-2.241	-2.99	-3.006	-2.926	-2.735	-2.808	-2.735	-2.914
	P-gp substrate	No	No	Yes	No	Yes	Yes	Yes	No
	P-gp I inhibitor	No	Yes	No	Yes	Yes	No	Yes	No
	P-gp II inhibitor	No	No	No	No	Yes	No	Yes	No
Distribution	VDss	0.128	0.296	0.058	0.198	-0.39	-0.386	-0.39	-0.565
	BBB permeability	0.163	-0.423	-0.629	-0.348	-1.066	0.42	-1.066	-0.05
	CNS permeability	-1.592	-2.178	-2.556	-2.135	-2.637	-2.047	-2.637	-2.215
Metabolism	CYP2D6 substrate	No	No	No	No	No	No	No	No
	CYP3A4 substrate	Yes	Yes	Yes	Yes	Yes	No	Yes	No
	CYP1A2 inhibitor	Yes	Yes	Yes	Yes	No	Yes	No	No
	CYP2C19 inhibitor	Yes	Yes	Yes	Yes	Yes	Yes	Yes	No
	CYP2C9 inhibitor	No	No	Yes	No	Yes	Yes	Yes	No
	CYP2D6 inhibitor	No	No	No	No	No	No	No	No
	CYP3A4 inhibitor	Yes	No	No	No	Yes	No	Yes	No
Excretion	Total Clearance	0.269	0.164	0.282	0.283	0.043	0.122	0.043	0.265
	Renal OCT2 substrate	No	No	No	Yes	No	No	No	No
Toxicity	AMES Toxicity	No	No	No	No	No	No	No	No
	Max. Tolerated dose	0.77	-0.341	-0.24	-0.111	-0.038	0.269	-0.038	-0.342
	hERG I inhibitor	No	No	No	No	No	No	No	No
	hERG II inhibitor	No	No	Yes	No	Yes	No	Yes	No
	Hepatotoxicity	No	Yes	No	No	Yes	No	Yes	No
	Skin Sensitisation	Yes	No	No	No	No	No	No	No

CONCLUSIONS

This study has successfully predicted the binding affinity, molecular dynamic simulation, and ADMET properties of secondary metabolites in *C. konishii* and *C. lucida*. Overall, ligands **5** and **7** show a better binding affinity due to the lower binding energy in molecular docking and molecular dynamic simulation. In ADMET properties calculation, both of ligands also fulfil parameters in adsorption and some of the parameters in distribution, metabolism, excretion, and toxicity test.

ACKNOWLEDGEMENTS

The authors thank Institute for Research and Community Service, Hasanuddin University for the research grant (No. 1476/UN4.22/PT.01.03/2022) in the scheme Academic Advisory Research in 2022.

REFERENCES

Chang, H.-S., Tang, J.-Y., Yen, C.-Y., Huang, H.-W., Wu, C.-Y., Chung, Y.-A., Wang, H.-R., Chen, I.-S., Huang, M.-Y., & Chang, H.-W. (2016).

Antiproliferation of *Cryptocarya concinna*-derived cryptocaryone against oral cancer cells involving apoptosis, oxidative stress, and DNA damage. *BMC Complementary and Alternative Medicine*, 16(1), 94. <https://doi.org/10.1186/s12906-016-1073-5>

Chou, T. H., Chen, J. J., Peng, C. F., Cheng, M. J., & Chen, I. S. (2011). New flavanones from the leaves of *cryptocarya chinensis* and their antituberculosis activity. *Chemistry and Biodiversity*, 8(11), 2015–2024. <https://doi.org/10.1002/cbdv.201000367>

Daina, A., Michielin, O., & Zoete, V. (2017). SwissADME: A free web tool to evaluate pharmacokinetics, drug-likeness and medicinal chemistry friendliness of small molecules. *Scientific Reports*, 7(January), 1–13. <https://doi.org/10.1038/srep42717>

Dash, R., Ali, M. C., Dash, N., Azad, M. A. K., Zahid Hosen, S. M., Hannan, M. A., & Moon, I. S. (2019). Structural and dynamic characterizations highlight the deleterious role

- of SULT1A1 R213H polymorphism in substrate binding. *International Journal of Molecular Sciences*, 20(24). <https://doi.org/10.3390/ijms20246256>
- Dassault Systemes. (2019). *Biovia Discovery Studio Visualizer*.
- de Kok, R. P. J. (2015). *Cryptocarya nitens* (Lauraceae), a new species record for Singapore. *Gardens' Bulletin Singapore*, 67(02), 253. <https://doi.org/10.3850/s2382581215000204>
- Feng, R., Guo, Z. K., Yan, C. M., Li, E. G., Tan, R. X., & Ge, H. M. (2012). Anti-inflammatory flavonoids from *Cryptocarya chingii*. *Phytochemistry*, 76, 98–105. <https://doi.org/10.1016/j.phytochem.2012.01.007>
- Gangopadhyay, M., & Chakrabarty, T. (2005). The Genus *Cryptocarya* R.Br. (Lauraceae) in the Indian Subcontinent. *Journal of Economic and Taxonomic Botany*, 29(2), 274–293.
- Gatoillat, G., Magid, A. A., Bertin, E., Btaouri, H. El, Morjani, H., Lavaud, C., & Madoulet, C. (2015). Medicarpin and millepurpan, two flavonoids isolated from *medicago sativa*, induce apoptosis and overcome multidrug resistance in leukemia P388 cells. *Phytomedicine*. <https://doi.org/10.1016/j.phymed.2015.09.005>
- Giordano, A., Fuentes-Barros, G., Castro-Saavedra, S., González-Cooper, A., Suárez-Rozas, C., Salas-Norambuena, J., Acevedo-Fuentes, W., Leyton, F., Tirapegui, C., Echeverría, J., Claros, S., & Cassels, B. K. (2019). Variation of secondary metabolites in the aerial biomass of *cryptocarya alba*. *Natural Product Communications*, 14(6), 1–11. <https://doi.org/10.1177/1934578X19856258>
- Hanwell, M. D., Curtis, D. E., Lonie, D. C., Vandermeersch, T., Zurek, E., & Hutchison, G. R. (2012). Avogadro: an advanced semantic chemical editor, visualization, and analysis platform. *Journal of Cheminformatics*, 4(17), 1–17.
- Juliawaty, L. D., Ra'idah, P. N., Abdurrahman, S., Hermawati, E., Alni, A., Tan, M. I., Ishikawa, H., & Syah, Y. M. (2020). 5,6-Dihydro- α -pyrones from the leaves of *Cryptocarya pulchinervia* (Lauraceae). *Journal of Natural Medicines*, 74(3), 584–590. <https://doi.org/10.1007/s11418-020-01397-7>
- Kitchen, D. B., Decornez, H., Furr, J. R., & Bajorath, J. (2004). Docking and scoring in virtual screening for drug discovery: methods and applications. *Nature Reviews Drug Discovery*, 3(11), 935–949. <https://doi.org/10.1038/nrd1549>
- Kurniadewi, F., Syah, Y. M., Juliawaty, L. D., Hakim, E. H., Koyama, K., & Kinoshita, K. (2017). Cytotoxic chalcones from some Indonesian *Cryptocarya*. *AIP Conference Proceedings*, 1862 (July 2017), 1–5. <https://doi.org/10.1063/1.4991189>
- Kurniadewi, Fera, Juliawaty, L. D., Syah, Y. M., Achmad, S. A., Hakim, E. H., Koyama, K., Kinoshita, K., & Takahashi, K. (2010). Phenolic compounds from *Cryptocarya konishii*: Their cytotoxic and tyrosine kinase inhibitory properties. *Journal of Natural Medicines*, 64(2), 121–125. <https://doi.org/10.1007/s11418-009-0368-y>
- Land, H., & Humble, M. S. (2018). YASARA: A Tool to Obtain Structural Guidance in Biocatalytic Investigations BT - *Protein Engineering: Methods and Protocols* (U. T. Bornscheuer & M. Höhne (eds.); pp. 43–67). Springer New York. <https://doi.org/10.1007/978-1-4939-7366-84>
- Liu, Y., Rakotondraibe, L. H., Brodie, P. J., Wiley, J. D., Cassera, M. B., Miller, J. S., Ratovoson, F., Rakotobe, E., Rasamison, V. E., & Kingston, D. G. I. (2015). Antimalarial 5,6-Dihydro- α -pyrones from *Cryptocarya rigidifolia*: Related Bicyclic Tetrahydro- α -Pyrones Are Artifacts. *Journal of Natural Products*, 78(6), 1330–1338. <https://doi.org/10.1021/acs.jnatprod.5b00187>
- Mark, P., & Nilsson, L. (2001). Structure and dynamics of the TIP3P, SPC, and SPC/E water models at 298 K. *Journal of Physical Chemistry A*, 105(43), 9954–9960. <https://doi.org/10.1021/jp003020w>
- Miller, B. R., Mcgee, T. D., Swails, J. M., Homeyer, N., Gohlke, H., & Roitberg, A. E. (2012). MMPBSA . py : An Efficient Program for End-State Free Energy Calculations. <https://doi.org/10.1021/ct300418h>
- Morris, G. M., Goodsell, D. S., Halliday, R. S., Huey, R., Hart, W. E., Belew, R. K., & Olson, A. J. (1998). Automated docking using a Lamarckian genetic algorithm and an empirical binding free energy function. *Journal of Computational Chemistry*, 19(14), 1639–1662. [https://doi.org/10.1002/\(SICI\)1096-987X\(19981115\)19:14<1639::AID-JCC10>3.0.CO;2-B](https://doi.org/10.1002/(SICI)1096-987X(19981115)19:14<1639::AID-JCC10>3.0.CO;2-B)
- Nasrullah, A. A., Zahari, A., Mohamad, J., & Awang, K. (2013). Antiplasmodial alkaloids from the bark of *Cryptocarya nigra* (Lauraceae). *Molecules*, 18(7), 8009–8017. <https://doi.org/10.3390/molecules18078009>
- Nehme, C. J., de Moraes, P. L. R., Tininis, A. G., & Cavalheiro, A. J. (2008). Intraspecific variability of flavonoid glycosides and styrylpyrones from leaves of *Cryptocarya mandiocana* Meisner (Lauraceae). *Biochemical Systematics and Ecology*, 36(8), 602–611. <https://doi.org/https://doi.org/10.1016/j.bse.2008.05.001>
- O'Boyle, N. M., Banck, M., James, C. A., Morley, C., Vandermeersch, T., & Hutchison, G. R. (2011). Open Babel: An open chemical toolbox. *Journal*

- of *Cheminformatics*, 3(33), 1–14. <https://jcheminf.biomedcentral.com/track/pdf/10.1186/1758-2946-3-33>
- Palestro, P. H., Gavernet, L., Estiu, G. L., & Blanch, L. E. B. (2014). Docking applied to the prediction of the affinity of compounds to P-glycoprotein. 2014.
- Pettersen, E., Goddard, T., Huang, C., Couch, G., Greenblatt, D., Meng, E., & TE, F. (2004). UCSF Chimera--a visualization system for exploratory research and analysis. *Journal of Computational Chemistry*, 25(13), 1605–1612.
- Pinzi, L., & Rastelli, G. (2019). Molecular docking: Shifting paradigms in drug discovery. *International Journal of Molecular Sciences*, 20(18). <https://doi.org/10.3390/ijms20184331>
- Pires, D. E. V., Blundell, T. L., & Ascher, D. B. (2015). pkCSM: Predicting small-molecule pharmacokinetic and toxicity properties using graph-based signatures. *Journal of Medicinal Chemistry*, 58(9), 4066–4072. <https://doi.org/10.1021/acs.jmedchem.5b00104>
- Pratama, M. R. F., Poerwono, H., & Siswodiharjo, S. (2020). ADMET properties of novel 5-O-benzoylpinostrobin derivatives. *Journal of Basic and Clinical Physiology and Pharmacology*, 30(6). <https://doi.org/10.1515/jbcpp-2019-0251>
- Rachman, M. M., Barril, X., & Hubbard, R. E. (2018). Predicting how drug molecules bind to their protein targets. *Current Opinion in Pharmacology*, 42, 34–39. <https://doi.org/10.1016/j.coph.2018.07.001>
- Ray, A., Jena, S., Sahoo, A., Kamila, P. K., Das, P. K., Mohanty, S., Nayak, S., & Panda, P. C. (2021). Chemical composition, antioxidant, anti-inflammatory and anticancer activities of bark essential oil of *Cryptocarya amygdalina* from India. *Journal of Essential Oil-Bearing Plants*, 24(3), 617–631. <https://doi.org/10.1080/0972060X.2021.1950051>
- Siallagan, J., Hakim, E. H., Syah, Y. M., Juliawaty, L. D., Achmad, S. A., Makmur, L., & Mujahidin, D. (2008). Secondary metabolites kurzichalcolactone A and B from *Cryptocarya lucida* Blume (Lauraceae). *The International Seminar on Chemistry*, 2008(October), 225–228.
- Usman, H., Hakim, E. H., Harlim, T., Jalaluddin, M. N., Syah, Y. M., Achmad, S. A., & Takayama, H. (2006). Cytotoxic chalcones and flavanones from the tree bark of *Cryptocarya costata*. *Zeitschrift Fur Naturforschung - Section C Journal of Biosciences*, 61(3–4), 184–188. <https://doi.org/10.1515/znc-2006-3-405>
- Wang, J., Wolf, R. M., Caldwell, J. W., Kollman, P. A., & Case, D. A. (2004). Development and testing of a general AMBER force field. *Journal of Computational Chemistry*, 25, 1157–1174.